



Research Article

Kinetics and Equilibrium Modeling of Single and Binary Adsorption of Aluminum(III) and Copper(II) Onto Calamansi (*Citrofortunella microcarpa*) Fruit Peels

Melanie G. Binauhan

Chemical Technology Examining Division, Bureau of Patents, Intellectual Property Office of the Philippines, Taguig, Philippines

Adonis P. Adornado

General Education Department, Colegio de Muntinlupa, Muntinlupa, Philippines

Lemmuel L. Tayo

School of Chemical, Biological, and Materials Engineering and Sciences, Mapua University, Manila, Philippines

Allan N. Soriano

Chemical Engineering Department, Gokongwei College of Engineering, De La Salle University, Manila, Philippines

Rugi Vicente C. Rubi*

Chemical Engineering Department, College of Engineering, Adamson University, Manila, Philippines

* Corresponding author. E-mail: rugi.vicente.rubi@adamson.edu.ph DOI: 10.14416/j.asep.2021.11.005
Received: 5 August 2021; Revised: 14 September 2021; Accepted: 21 September 2021; Published online: 15 November 2021
© 2021 King Mongkut's University of Technology North Bangkok. All Rights Reserved.

Abstract

The introduction of heavy metal wastes in the environment has posed health risks to both human and animals due to their toxicity. Since then, different studies have been explored for the possibility of utilizing new, low-cost, and sustainable adsorbent materials to get rid of heavy metals in the wastewater streams and aqueous solutions. This present study aimed to investigate and compare the adsorption ability of powdered calamansi (*Citrofortunella microcarpa*) fruit peels (PCFP) for the elimination of both Al(III) and Cu(II) ions in single (non-competitive) and binary (competitive) aqueous systems by batch adsorption techniques. Scanning electron microscopic and spectroscopic techniques were used to characterize the surface morphologies for the biosorbent and quantify the removal rates of heavy metal, respectively. Models were then used to describe in detail about the adsorption kinetics and isotherms for both single and binary metal systems. The influence and dependency of different experimental conditions on adsorption performance were also analyzed. The PCFP derived biosorbent was successful in removal of both Al(III) and Cu(II) ions in single (non-competitive) and binary (competitive) aqueous systems with 99, 70, and 91% adsorption rates, respectively. The biosorption process follows the Ho's pseudo-second order kinetics. Furthermore, the Langmuir isotherm model was found helpful in explaining the adsorption mechanism. The dominating electrostatic interaction between adsorbents and adsorbates demonstrates monolayer adsorption at the binding sites on the surface of the peeling. Finally, the findings of this study will contribute to a better understanding of the adsorption process, as well as future system design applications in the treatment of heavy metal containing waste effluents.

Keywords: *Citrofortunella microcarpa*, Biosorption, Adsorption kinetics, Isotherm models, Heavy metals, Binary metal system

1 Introduction

Water contamination has been known to be aggravated by rapid population and industrial development. One particular concern is the contamination of the bodies of water with toxic heavy metals that posed a challenge to scientists and engineers. Heavy metals, unlike most emerging pollutants, are recalcitrant and cannot be decomposed or detoxified biologically [1]. Therefore, wastewater containing heavy metals must be disposed in a safe, efficient, and environmentally friendly way. However, manufacturers and environmentalists have difficulty because no cost-effective remediation options are available. Furthermore, some successful heavy metals removal technologies are still in their initial stages.

Some metals are known to be susceptible to bioaccumulation in biological organisms. When the tolerated limitations for adsorption in the body are exceeded, it becomes toxic. Typically known ecotoxicological hazardous metals include the following: aluminium (Al), antimony (Sb), cadmium (Cd), chromium (Cr), copper (Cu), lead (Pb), manganese (Mn), and mercury (Hg) [2]–[4]. For example, Al and its alloys are commonly used in the construction parts of aircraft vehicles, motor bases, and utensils. This is due to its strength, durability, and being lightweight. Despite these benefits, adverse effects of Al have been reported. Al has been shown to be a neurotoxic compound if it enters the bloodstream. In addition, Al has been linked to Alzheimer's and Lou Gehrig's diseases, and other kinds of advanced dementia [2].

Likewise, Cu is a commonly used material in our daily life. The primary application is in cleaning and plating metals, pulp and paper industry, and as fertilizer additive [3]. Also, Cu can also be found in foods like shellfish, liver, mushrooms, almonds, and chocolate [4], [5]. Even though Cu is necessary to human life and health, it is potentially toxic as well in an excessive amount. Continuous inhalation of Cu-containing sprays has been related to lung cancer and liver diseases. Even at relatively low quantities in natural water, it is harmful to aquatic organisms [6].

To address this dilemma, various physico-chemical technique such as cementation, pH adjustments, electrode deposition, evaporation, ion-exchange, ultrafiltration, reduction, reverse osmosis, and

selected solvent extraction has been conducted [7]–[9]. However, the major drawback of these methods is high operational costs or insufficiency to meet regulatory requirements. Thus, adsorption is a promising alternative process of heavy metals removal. This is due to high efficiency heavy metal removal, low operating cost, and minimized volume of chemical consumption [10]. The typical adsorption process for heavy metals removal utilized activated carbon as an adsorbent [11], [12]. Likewise, biosorption is an emerging technique of heavy metal removal that utilized biosorbent derived from natural materials [13]. Typically, a low-cost adsorbent is preferred to minimize operating cost. Adsorbents that are low-cost are those that involve minimum preparation, are available in nature, or are a by-product from another sector. Recently, different researches have been dedicated to the development of low-cost activated carbon adsorbents from cheaper materials [14]. Various sources ranging from agricultural wastes [15], clay minerals [16], and food wastes [17] are employed in the elimination of heavy metals.

There has been a huge amount of low-cost adsorbents production from food sources as applied to heavy metals removal in waste streams. To the best of the authors' knowledge, few were actually tested and published in the literature for the adsorption of heavy metals for single and binary Al(III) and Cu(II) using powdered calamansi (*Citrofortunella macrocarpa*) fruit wastes peels as an adsorbent.

Locally known as “Kalamansi”, it is an indigenous and among the most widely cultivated fruit crop in the Philippines and distributed in Southeast Asia. Other common names for this species include calamodin, kalamondin, kalamunding, and limonsito. It is a member of the Rutaceae family. It is an intergenetic cross between *Citrus reticulata*, or “tangerine”, and *Fortunella japonica*, or “oval kumquat.”

Recently, Sumalapao *et al.* [18] explored the adsorptive properties of unripe *C. microcarpa* fruit peels on the elimination of congo red (a diazo dye) from the derived aqueous solution in a single component adsorption system [18]. A prior similar study was done by Agboinghale [19], but he made use of orange fruit peels, which belong to the same family. In addition, the adsorption properties, mechanisms, and phenomena involved in heavy metal removal onto *C. microcarpa* fruit peels have been seldom studied, and no attempt was done to analyze the system in terms

of binary sorption isotherms.

Meanwhile, adsorption processes that utilize adsorbents from natural waste materials have proven to be more advantageous over synthetic adsorbents. This is due to its low operational cost and sustainability.

Thus, the objective of this study is to present the adsorption ability of Powdered Calamansi (*Citrofortunella microcarpa*) fruit peels (PCFP) for the removal of both Al(III) and Cu(II) ions in single (non-competitive) and binary (competitive) aqueous systems. A batch adsorption test will be performed to determine the optimum removal conditions. In addition, the isothermal and kinetic study will be applied to establish the removal mechanism.

2 Methods

2.1 Chemicals used

In this study, preparation of the adsorbent and succeeding experimental runs were done using an analytical reagent (AR) grade chemicals of aluminum nitrate ($\text{Al}(\text{NO}_3)_3 \cdot 9\text{H}_2\text{O}$) and copper nitrate ($\text{Cu}(\text{NO}_3)_2 \cdot 2.5\text{H}_2\text{O}$). These chemicals were procured from Belman Laboratories, Mandaluyong, Philippines, and used as purchased.

The prepared stock solutions for single and binary Al(III) and Cu(II) were performed based on the works of Wong *et al.* [20] by completely dissolving 0.2524 g of $\text{Al}(\text{NO}_3)_3 \cdot 9\text{H}_2\text{O}$ and 0.2528 g $\text{Cu}(\text{NO}_3)_2 \cdot 2.5\text{H}_2\text{O}$ in appropriate amounts of distilled water. Then the mixture was diluted to produce the experimental single and binary Al(III) and Cu(II) solutions of desired concentrations of 2.33 mg/L and 1.65 mg/L, respectively. Then, all prepared stock solutions were acidified with concentrated hydrochloric acid ($\text{HCl}_{(aq)}$) to prevent hydrolysis and maintained at $\text{pH} = 6$.

2.2 Biosorbent preparation

For this study, 30 kg of unripe *C. microcarpa* [Figure 1(a)] was procured from Balintawak Public Market, Quezon City, Philippines. A representative sample was taxonomically identified at the Bureau of Plant Industry, Manila, Philippines. The mature fruits (diameter = 33 to 35 mm) were subsequently peeled-off manually. To eliminate clinging dirt and other foreign contaminants, the fruit peels were



Figure 1: (a) Mature calamansi (*C. macrocarpa*) sample, (b) dried and finely grind calamansi (*C. macrocarpa*) sample.

thoroughly washed three times with distilled water, and then cut into small pieces (10 to 20 mm). Then the sample was air-dried for about 12 days at an average ambient temperature of 34 °C and relative humidity of 69%. This sample was redried in a forced air-drying oven (Model: SM01 by Shel Lab®, Oregon, USA) at 100 °C for 90 min and finely grounded [Figure 1(b)]. The individual masses of the fresh and dried fruit peel, on average, were taken to be 3.9600 g and 1.1944 g, respectively, using an ATX Series Analytical Balance (Model: ATX224, Shimadzu, Kyoto, Japan) with a standard deviation of ≤ 0.1 mg. This process accounts for about 69.84% mass reduction due to moisture loss. The dried fruit peels were then crushed and ground [Figure 1(b)] using Wiley mill (Thomas Scientific, New Jersey, USA). To control the particle size, the ground fruit peels were then screened and sieved (mesh no. 120) to an approximate size of 125 μm . Deteriorated cells have a greater accessible surface area and intracellular component, which increases the number of surface binding sites available and changes the functional groups in the cell wall [21]. The filtered particles were then collected in a clear wide-mouth reagent bottle and kept in a desiccator until they were utilized in the batch adsorption experiment.

2.3 Batch adsorption experiments

The adsorption experimental set-up was performed in 125 mL Erlenmeyer flasks and equilibrated at 37 ± 0.2 °C using a shaking incubator (BAE07-H300, FINEPCR®, FINEPCR Co., Ltd., Gyeonggi-do, Korea) at a constant agitation rate of 110 ± 2 rpm. The effects of agitation time with varying biosorbent dosage on the initial concentration of single and binary Al(III) and

Cu(II) and the percentage removal were investigated by the agitation of 25 mL aliquot of 2.33 mg/L Al(III) / 1.65 mg/L Cu(II) with 0.25, 0.50, 1.00 and 2.00 g adsorbent dosage of size 125 μm for 12 h. For every set time durations of (30, 60, 180, 360 and 720 min), the samples were filtered using Whatman® Ashless Grade 40 Filter Paper (pore size 8.00 μm) to remove the adsorbent from the solution. The filter cake which contains the biosorbent was dried in a forced air-drying oven (Model: SM01 by Shel Lab®, Oregon, USA) at 50 °C until all moisture content were evaporated. While the filtrate which contained single and binary Al(III) and Cu(II) remaining in the solution was then acid digested.

Furthermore, in a 250 mL beaker, acid digestion was initiated by adding 2 mL of concentrated nitric acid ($\text{HNO}_{3(\text{aq})}$) to the filtrate and then covered with a watch glass. The mixture was boiled gently on a hot plate until the total volume decreased by 75%. After cooling, another 2 mL concentrated $\text{HNO}_{3(\text{aq})}$ was added, followed by further heating until total digestion was achieved. The digested filtrate samples were set aside for spectrophotometric analysis of residual concentrations of single and binary Al(III) and Cu(II). Using running blank tests, it was discovered that the adsorption of single and binary Al(III) and Cu(II) on the walls of flasks glass and funnel tubes were insignificant. The same analytical procedures were used in the subsequent experiments. All experimentation in this study was carried out in triplicates.

The calculation for the adsorption capacity (q_e) of calamansi biosorbent on the single and binary Al(III) and Cu(II) at equilibrium can be derived from Equation (1). This is dependent on the difference of single and binary Al(III) and Cu(II) concentration before and after adsorption, the aqueous solution's volume, and the amount of the biosorbent.

$$q_e = \frac{(C_o - C_e)V}{M} \cdot \frac{1}{1000} \quad (1)$$

where C_o and C_e is the initial single and final binary Al(III) and Cu(II) concentration (mg/L), V is the solution's volume (mL) and M (g) as the amount of the PCFP (biosorbent) used. The effects of the amount of PCFP in the single and binary metal ions can be verified using Equation (2). The initial and final concentrations of single and binary Al(III) and Cu(II), is expressed as C_i and C_f (mg/L) respectively [22].

$$\% \text{Removal} = \frac{(C_i - C_f)}{C_i} \cdot 100 \quad (2)$$

2.4 Characterization

The morphological properties of the untreated (before) and treated (after) PCFP were established using a benchtop Scanning Electron Microscope (SEM) (TM4000Plus, Hitachi High-Technologies, Tokyo, Japan). The SEM used was also coupled with a built-in type detector Energy Dispersive X-ray Spectrometer (EDX/S, Model: Quantax75, Bruker Nano GmbH, Massachusetts, USA) to confirm the presence and quantify the amount of the heavy metal ions onto PCFP surface by weight distribution. The SEM-EDX results were also used to detect the metal sorption regions on the PCFP [23]. Similarly, the quantities of single and binary Al(III) and Cu(II) in controlled and experimental samples were determined using tabletop, dual-view Inductively Coupled Plasma – Optical Emission Spectrometry (ICP-OES, Optima™ 8000, PerkinElmer, Massachusetts, USA). The standard concentrations for Cu(II) and Al(III) binary solutions is at the range of 0.5 to 10 mg/L. The detection limit is set to 0.020 mg/L for Al(III) and 0.005 mg/L for Cu(II). Finally, an optimum wavelength of 396.153 nm and 327.393 nm for Al(III) and Cu(II) were set, respectively.

2.5 Adsorption kinetic studies

To understand the mechanism between the adsorbate-adsorbent sorption interaction, numerous kinetic models have been developed [24], [25]. It is known that the relationship between contact time and the amount of metals adsorbed depicts a chaotic non-linear interacting relationship. The pseudo-first and -second order kinetic models were utilized to process the experimental data. This is important in the understanding of the governing mechanism of adsorption processes, such as mass transfer and chemical reaction [26], [27].

Lagergren's Pseudo-First Order Kinetic Model. Shown in Equation (3) is the pseudo-first order kinetic model, which is a typical adsorption kinetic analysis [28], [29] for adsorption process.

$$\frac{dq_t}{dt} = k_1(q_e - q_t) \quad (3)$$

where q_e (mg/g), adsorption performance in equilibrium.

The q_t (mg/g) is adsorbed amount of single and binary metals at a certain time t (min). Also, k_1 (min^{-1}) is the adsorption rate constant. The linearized form of this model of Equation (3) is shown in Equation (4),

$$\log(q_e - q_t) = \log q_e - \frac{k_1 t}{2.303} \quad (4)$$

Ho's Pseudo-Second Order Kinetic Model. This model is frequently used to describe and evaluate the kinetics of adsorption in diverse adsorption systems [30], [31]. This was represented in Equation (5),

$$\frac{dq_t}{dt} = k_2 (q_e - q_t)^2 \quad (5)$$

where q_e (mg/g) is adsorption performance in equilibrium. The q_t (mg/g) is adsorbed amount of single and binary metals at a certain time t (min). Also, k_2 (min^{-1}) is the adsorption rate constant in ($\text{g/mg} \cdot \text{min}$). The linearized form to this second order differential equation is in Equation (6),

$$\frac{t}{q_t} = \frac{1}{k_2 q_e^2} + \frac{t}{q_e} \quad (6)$$

2.6 Adsorption equilibrium studies

The understanding of the sorption phenomena as described by various adsorption isotherms is typically based on three criteria. First, the adsorbate-adsorbent interaction per unit mass. Then, the well-established the equilibrium between heavy metal ions on the available surface of the sorbent. Lastly, the unadsorbed metal ions in the aqueous solution. These are measured to determine the adsorption efficiency of the biosorbent as applied to heavy metal ions. The Langmuir and Freundlich models were employed in this study to examine the biosorption isotherms [32].

Langmuir Adsorption Isotherm Model. In this model, the adsorption phenomenon develops at energetically identical particular homogeneous active sites. Likewise, saturation is obtained when the heavy metal ions are adhered to the structurally homogenous sites. In this case, adsorption is no longer possible. Furthermore, as the molecules deviate from the adsorption surface, the molecular force of attraction decreases rapidly [33]. The Langmuir isotherm is presented in Equation (7),

$$q_e = \frac{q_m K_L C_e}{1 + K_L C_e} \quad (7)$$

where q_e (mg/g) is adsorption performance in equilibrium. The maximum monolayer adsorbent capacity q_m is in mg/g. Also, the equilibrium adsorbate concentration, C_e is in mg/L. On the other hand, the Langmuir equilibrium constant, K_L (L/mg) is related to the affinity and heat of adsorption. The linearized form of this model determines the constants K_L and q_m as presented in Equation (8),

$$\frac{1}{q_e} + \frac{1}{q_m} + \frac{1}{q_m K_L C_e} \quad (8)$$

Freundlich Adsorption Isotherm Model. This model is the best to represent the adsorption of adsorbate onto heterogeneous surfaces. Here, stronger active sites for binding are occupied first, and as the number of occupied sites increases, the binding affinity diminishes [34]. The model isotherm is expressed in Equation (9),

$$q_e = K_F C_e^{1/n} \quad (9)$$

where q_e (mg/g) is the amount of heavy metals adsorbed and C_e (mg/L) is the adsorbate concentration, determined at equilibrium condition. In addition, the measured adsorbent capacity, K_F is in the form of ($\text{mg/g} \cdot (\text{L/mg})^n$). The expression $1/n$ is sorption intensity. The linearized form of this model [35] which includes the is parameters K_F and n presented in Equation (10).

$$\log q_e = \log K_F + \frac{1}{n} \log C_e \quad (10)$$

3 Results and Discussion

3.1 Effect of adsorption time and biosorbent dosage on the removal of single and binary Al(III) and Cu(II) onto powdered calamansi (*Citrofortunella microcarpa*) fruit peels (PCFP)

Figures 2–4 describe the influence of adsorption time and varying biosorbent dosage on the percentage removal of single and binary Al(III) and Cu(II) onto PCFP. The single and binary uptake of Al(III) and Cu(II) continues to increase up to a certain threshold. Once this limit was achieved, no further changes was observed. Also, the enhanced sorption phenomenon at the surface sites is attributed to the increase of biosorbent dosage.

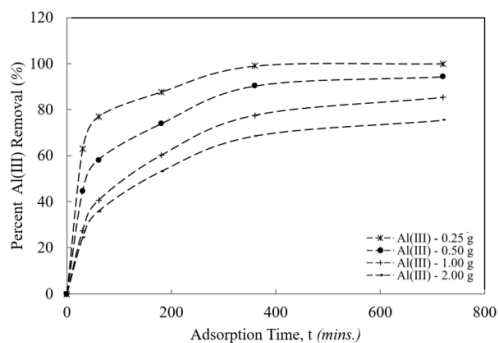


Figure 2: Effect of adsorption time and biosorbent dosage on the removal of Al(III) onto powdered calamansi (*Citrofortunella microcarpa*) fruit peels (PCFP) (Conditions: agitation speed = 110 ± 2 rpm; pH_i = 6; $C_{Al(III)i}$ = 2.33 mg/L; $C_{Cu(II)i}$ = 1.65 mg/L; particle size = 125 μ m; $T = 37 \pm 0.2$ °C; $V = 25$ mL)

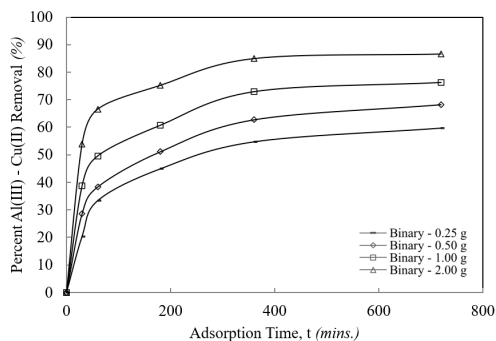


Figure 4: Effect of adsorption time and biosorbent dosage on the removal of binary Al(III) and Cu(II) onto powdered calamansi (*Citrofortunella microcarpa*) fruit peels (PCFP) (Conditions: agitation speed = 110 ± 2 rpm; pH_i = 6; $C_{Al(III)i}$ = 2.33 mg/L; $C_{Cu(II)i}$ = 1.65 mg/L; particle size = 125 μ m; $T = 37 \pm 0.2$ °C; $V = 25$ mL)

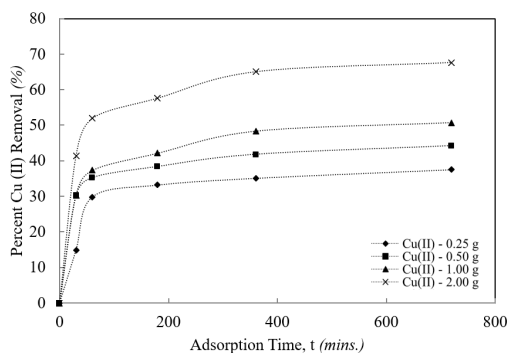


Figure 3: Effect of adsorption time and biosorbent dosage on the removal of Cu(II) onto powdered calamansi (*Citrofortunella microcarpa*) fruit peels (PCFP) (Conditions: agitation speed = 110 ± 2 rpm; pH_i = 6; $C_{Al(III)i}$ = 2.33 mg/L; $C_{Cu(II)i}$ = 1.65 mg/L; particle size = 125 μ m; $T = 37 \pm 0.2$ °C; $V = 25$ mL)

Likewise, heavy metal saturation at the surface is associated to the increase in adsorption time. This denotes higher heavy metals sorption at the beginning of the adsorption process. The available surface area of the PCFP biosorbent at the start of the adsorption process facilitates a faster adsorption phenomenon. When the adsorption sites are saturated, the uptake pace is controlled by the transport rate of the heavy metal ions from the surface to the inner part of the biosorbent [8]. Therefore, the higher amount of adsorbent present in the aqueous solution, the higher is the number of adhering adsorbent particles in the heavy metals [36].

It was observed that the mean removal of single and binary Al(III) and Cu(II) revealed a rapid initial adsorption in the first 30 min interval. Beyond the first pre-determined time interval, the adsorption or removal rate gradually increases. It was slowed down until it almost reached equilibrium at 400 min and eventually remains constant up to 720 min. In addition, the maximum percent heavy metal ion removal was attained at 540 min of stirring time. Therefore, the equilibrium contact time was set at this time for all biosorbent. The moderate adsorption rate is attributed to the repulsive force of interaction between heavy metal molecules in the solid and bulk region. It was noticeable that PCFP showed a good adsorption for Al(III) ions compared to Cu(II) in single component system. This observation is associated with competitive heavy-metal ion adsorption in the multi-metal system. In addition, the phenomenon is affected by electrostatic interaction, affinity, and selectivity between the interacting materials. It was observed that there is a generally close adsorption curve for a single metal system of Al(III) and Cu(II) ions.

Contrarily, the obtained adsorption isotherms for binary metals systems exhibit a higher gap curve behavior. This is attributed to the competitive interaction between solute-solute and surface-solute region. It was found out that in a competitive scenario, Cu(II) has a higher adsorption preference than Al(III). Also, heavy metals influx in the biosorbent surface is exhibited by a

smooth, single, and continuous curve [37]. Increasing the amounts of biosorbents used increases the removal performance of single and binary Al(III) and Cu(II). Hence, a decreasing biosorbent dosage corresponds to the decreases in the removal performance of the heavy metals. This is associated to the reverse adsorption trends due to rapid adsorption of all available sites [38].

The percentage removal of single and binary heavy metal ions remarkably increases at an increasing biosorbent dosage. An increase in the biosorbent dosage from 0.25 g to 2.00 g resulted in an average 25–45% increase in the percent removal. It is clear that as the dosage of PCFP increases, the percent elimination of heavy metal ions increases rapidly. This is attributed to larger accessible surface sites for adsorption [39]. This increase in biosorbent’s adsorptive region promotes the heavy metal ion attachment in the sorption sites [40], [41].

3.2 SEM–EDX/S analyses of untreated (Before) and treated (After) PCFP

The SEM micrographs of PCFP before sorption of single and binary metals of Al(III) and Cu(II) were shown in Figure 5(a). It can be noticed that the surface of PCFP showed a crumbly irregular morphology, which is typical with plant-based cellulosic materials [42], [43].

In contrast, Figure 5(a)–(e) showed the SEM micrographs of PCFP after the binary Al(III) and Cu(II) sorption a denser surface morphology. The structural changes at the biosorbent surface are primarily influenced by the presence of Al(III) and Cu(II) ions. This was exhibited with the white crystalline areas that contain most of the sorbed metal. In Figure 5(c)–(e), Al(III) ions can be spotted in the electron micrograph as the blurred circular crystals adhering to the surface of PCFP. On the longitudinal flake crystals of Cu(II) ions were observed. Also, as shown in the EDX analysis the predominant deposition of Cu(II) in the PCFP biosorbent at different surface sites was obtained. In fact, Figure 5(c) (surface site 1) revealed the weight distribution for Al(III) and Cu(II) ions of 15.09% and 84.91%, respectively. While, Figure 5(d) (surface site 2) exhibited a weight distribution is 28.72% and 71.28%, respectively. Finally, Figure 5(e) (surface site 3) the percentage of Al(III) is 20.00% while 80.00% for Cu(II).

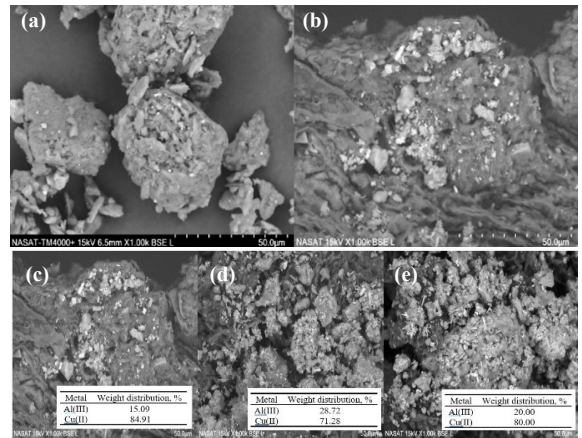


Figure 5: SEM micrographs of (a) Untreated (Before) and (b) Treated (After) powdered calamansi (*Citrofortunella microcarpa*) fruit peels (PCFP) (Magnification: X1.00k), SEM–EDX analysis of used PCFP biosorbent at different surface sites (c), (d), and (e) (Magnification: X1.00k).

3.3 Modeling of adsorption kinetics

For the various non-linear kinetic models used in this work, initial parameter estimations were derived. The respective linearized form is presented in Equations (4) and (6). In the pseudo-first order kinetic model, the line plots of $\log(q_e - q_t)$ versus the time, t are reflected in Figure 6. Also, presented in Table 1, are the values of k_1 and q_e for pseudo-first order kinetic model. These parameters were computed using the slope and the intercept of the obtained straight-line graph derived from the model.

Table 1: Constants and correlation coefficients for pseudo-first and -second order isotherms for the adsorption of single and binary Al(III) and Cu(II) onto powdered Calamansi (*Citrofortunella microcarpa*) fruit peels (PCFP)

System	Pseudo-First Order Kinetic Model		
	q_e (mg/g)	k_1 (min ⁻¹)	R^2
Single Al(III)	0.0109	0.0074	0.9602
Single Cu(II)	0.0045	0.0051	0.9401
Binary, Al(III)-Cu(II)	0.0094	0.0016	0.8112
System	Pseudo-Second Order Kinetic Model		
	q_e (mg/g)	k_1 (min ⁻¹)	R^2
Single Al(III)	1.3067	0.0205	0.9990
Single Cu(II)	0.8641	0.0449	0.9993
Binary, Al(III)-Cu(II)	1.0842	0.0288	0.9993

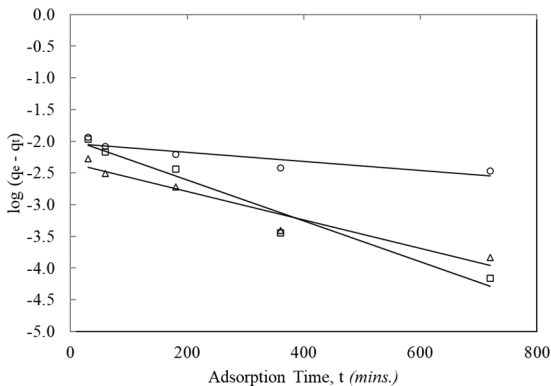


Figure 6: Pseudo-first order kinetic plot of (□) single Al(III), (△) single Cu(II), and (○) binary Al(III) and Cu(II) adsorbed onto powdered calamansi (*Citrofortunella microcarpa*) fruit peels (PCFP) (symbols represent the experimental data points and solid lines are calculated model).

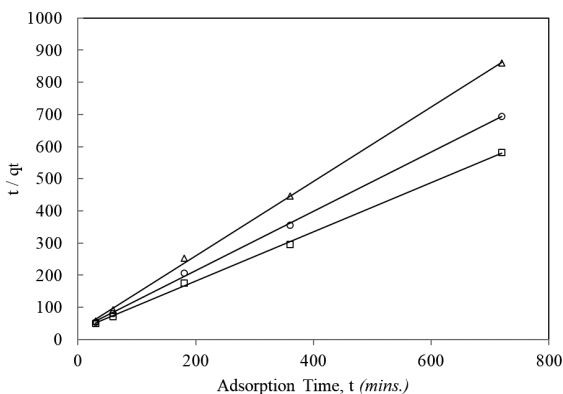


Figure 7: Pseudo-second order kinetic plot of (□) single Al(III), (△) single Cu(II), and (○) binary Al(III) and Cu(II) adsorbed onto powdered calamansi (*Citrofortunella microcarpa*) fruit peels (PCFP).

Also, it was found out that the computed q_e based on the line plots are deviating from the observed values. Since, the coefficient of determination (R^2) is not equal to 1, the adsorption phenomenon cannot be adequately described using the pseudo-first order adsorption model equation. Meanwhile, Figure 7 shows the linear plots of t/q_t versus t for pseudo-second order kinetic model. The computed values of the rate constant, k_2 , and capacity, q_e , at equilibrium were derived using the slope and intercept parameters as

depicted in Table 1. Noticeably, the q_e showed a little deviation ($R^2 = 0.99$) between observed and predicted values when using the pseudo-second order kinetic model. This result suggested that the pseudo-second order kinetic model equation was an appropriate modeling tool to describe the current adsorption phenomenon.

This indicates that the governing sorption mechanism for single and binary Al(III)–Cu(II) adsorption phenomenon is described by the pseudo-second order model. Here, adsorption rate is directly related to the square of the available sites [42]. This suggests that the biosorption of Al(III) and Cu(II) on PCFP was based on a chemical reaction. This occurred with the interaction of the heavy metal ions and the biosorbent's active sites.

3.4 Modeling of adsorption isotherms

To determine the sorption process behavior of the heavy metal ions in both single and binary metal systems, the Langmuir and Freundlich isotherm models were used. Typically, the governing driving force interaction between the adsorbate–adsorbent is necessary for the optimization of adsorption process.

Presented in Equation (8) is the Langmuir adsorption isotherm model used in this study. Furthermore, presented in Figure 8 is the linear plots of $1/C_o$ versus $1/q_e$. The values of the parameters (Table 2), such as the energy of adsorption, K_L , and adsorption capacity, q_m , were derived using slope and intercept of the plot. On the other hand, presented in Figure 9 is the line plots of $\log C_e$ versus $\log q_e$ using the Freundlich adsorption isotherm model as described by Equation (9). Here, the parameters, $1/n$ (slope) and $\log K_F$ (intercept), are given in Table 2.

The distinguishing indicator for the evaluation of Langmuir isotherm can be represented R_L , which is a dimensionless parameter or separation factor at equilibrium condition. This can be used to predict if a system is “favorable” or “unfavorable” for adsorption phenomenon [42]. Here, R_L (separation factor) can be calculated using Equation (11),

$$R_L = \frac{1}{1 + K_L C_o} \quad (11)$$

where C_o is the initial Al(III) and Cu(II) concentration in the solution (mg/L) and K_L is the adsorption

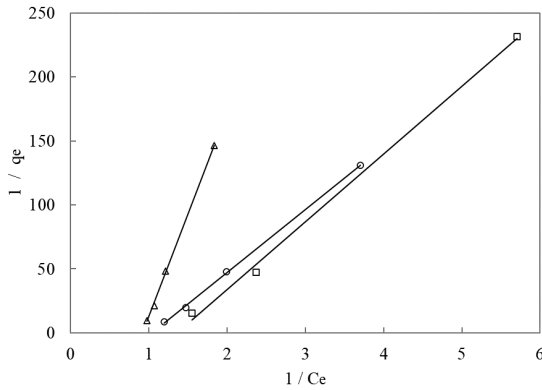


Figure 8: Langmuir adsorption isotherm for the removal of (□) single Al(III), (△) single Cu(II), and (○) binary Al(III) and Cu(II) onto powdered calamansi (*Citrofortunella microcarpa*) fruit peels (PCFP).

Table 2: Langmuir and freundlich isotherm model constants and correlation coefficients for the adsorption of single and binary Al(III) and Cu(II) onto powdered calamansi (*Citrofortunella microcarpa*) Fruit Peels (PCFP)

System	Langmuir Constants			
	q_m (mg/g)	K_L (L/mg)	R^2	R_L
Single Al(III)	0.0140	1.3533	0.9974	0.2408
Single Cu(II)	0.0068	0.9189	0.9990	0.3184
Binary Al(III)-Cu(II)	0.0195	1.0417	0.9996	0.2918
System	Freundlich Constants			
	$1/n$	K_F (mg/g)(L/mg) ⁿ	R^2	
Single Al(III)	2.0331	0.1418	0.9907	
Single Cu(II)	1.7318	0.0660	0.9229	
Binary Al(III)-Cu(II)	2.3346	0.1400	0.9577	

equilibrium constant or Langmuir isotherm model (L/mg). Here, the R_L depicts the adsorption process condition and can be interpreted as follows:

- (i) Not favorable if $R_L > 1$
- (ii) Linear if $R_L = 1$
- (iii) Favorable if $0 < R_L < 1$
- (iv) Irreversible if $R_L < 0$

As shown in Table 2, the value of separation factor for single Al(III) ($R^2 = 0.2408$), Cu(II) ($R^2 = 0.2408$) and binary Al(III)–Cu(II) ($R^2 = 0.2019$) indicates a favorable adsorption system.

On the other hand, for Freundlich isotherm, the value of n obtained was in the ranges from 1 to 10.

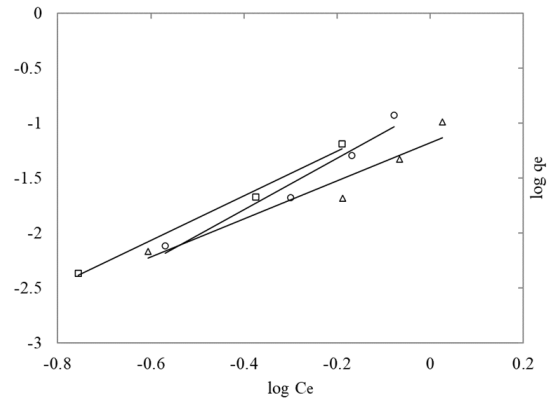


Figure 9: Freundlich adsorption isotherm for the removal of (□) single Al(III), (△) single Cu(II), and (○) binary Al(III) and Cu(II) onto powdered calamansi (*Citrofortunella microcarpa*) fruit peels (PCFP) (symbols represent the experimental data points and solid lines are calculated model).

This indicates a good adsorbate–adsorbent interaction [44]. On the other hand, the value of the expression, $1/n$ showed an indication of a favorable sorption phenomenon. While, getting the values of $n > 1$ exhibits a favorable sorption condition. The adsorption intensity (L/mg) is dependent on the temperature and characteristics of the adsorbate and adsorbent, as indicated by the empirical constant.

Here, the computed n for the removal of single Al(III) ($n = 0.4919$), Cu(II) ($n = 0.5774$) and binary Al(III)–Cu(II) ($n = 0.4283$) indicates a non–favorable adsorption condition when using the Freundlich isotherm model. Also, the biosorption process when using Langmuir equation was well–correlated ($R^2 > 0.99$), which supports the experimental data obtained. This is better than using the Freundlich equation with ($R^2 > 0.96$). This indicates that the metal ions sorbed on the adsorbent surface that formed a monolayer. Furthermore, the equilibrium data as given by the Freundlich equation is attributed to the true heterogeneity of the metal uptake surface locations [45]. Generally, Langmuir isotherm model seemed to be a better modeling tool than that of Freundlich model.

The possible reason is the Langmuir isotherm is known to correspond to a prominent ion exchange process. The Freundlich isotherm, on the other hand, depicts adsorption–complexation reactions in the adsorption process.

4 Conclusions

The produced powdered calamansi (*Citrofortunella microcarpa*) fruit peels (PCFP) showed potential as a low cost and efficient biosorbent for the individual and simultaneous eliminations of Al(III) and Cu(II) ions. It was found out that the heavy metal removal rates were in the ranges of 68–100%. In addition, the adsorption was primarily affected by the initial Al(III) and Cu(II) concentrations, adsorbent dosage, and contact time. The biosorbent capacity increases as the adsorption time and sorbent dosage increases. It was also observed that the rapid heavy metal removal occurred at the beginning of the adsorption process. This observation was then followed by gradually decline in the adsorption capacity. It then reached saturation at equilibrium condition indicating a cessation of adsorption process. The kinetics of adsorptions for single and binary Al(III) and Cu(II) onto PCFP follow Ho's pseudo-second order kinetics. The elimination of single and binary Al(III) and Cu(II) using PCFP is better fitted when using Langmuir isotherm than Freundlich models. This shows that at the surface's binding sites of the biosorbent from calamansi peels, monolayer adsorption occurs is dominated by adsorbent-adsorbate electrostatic interaction. Finally, the results obtained in this study will provide insights into adsorption mechanism and phenomena involved in wastewater containing heavy metals.

References

- [1] N. P. Cheremisinoff, *Handbook of Water and Wastewater Treatment Technologies*. Oxford, England: Butterworth-Heinemann, 2002.
- [2] Y. Nuhoglu and E. Oguz, "Removal of copper(II) from aqueous solutions by biosorption on the cone biomass of *Thuja orientalis*," *Process Biochemistry*, vol. 38, pp. 1627–1631, 2003.
- [3] R.-S. Juang and H.-J. Shao, "Effect of pH on competitive adsorption of Cu(II), Ni(II), and Zn(II) from water onto chitosan beads," *Adsorption*, vol. 8, pp. 71–78, 2002.
- [4] A. V. AjayKumar, N. A. Darwish, and N. Hilal, "Study of various parameters in the biosorption of heavy metals on activated," *World Applied Sciences Journal*, vol. 5, pp. 32–40, 2009.
- [5] L. Wartelle and W. Marshall, "Citric acid modified agricultural by-products as copper ion adsorbents," *Advances in Environmental Research*, vol. 4, pp. 1–7, 2000.
- [6] S. Al-Asheh, F. Banat, and F. Mohai, "Sorption of copper and nickel by spent animal bones," *Chemosphere*, vol. 39, pp. 2087–2096, 1999.
- [7] J. W. Patterson, *Industrial Wastewater Treatment Technology*. Oxford, England: Butterworth-Heinemann, 1985.
- [8] B. Yu, Y. Zhang, A. Shukla, S. S. Shukla, and K. L. Dorris, "The removal of heavy metal from aqueous solutions by sawdust adsorption—removal of copper," *Journal of Hazardous Materials*, vol. 80, pp. 33–42, 2000.
- [9] S.-H. Lin and R.-S. Juang, "Heavy metal removal from water by sorption using surfactant-modified montmorillonite," *Journal of Hazardous Materials*, vol. 92, pp. 315–326, 2002.
- [10] S. Babel and T. A. Kurniawan, "Low-cost adsorbents for heavy metals uptake from contaminated water: A review," *Journal of Hazardous Materials*, vol. 97, pp. 219–243, 2003.
- [11] A. Baçaoui, A. Yaacoubi, A. Dahbi, C. Bennouna, R. P. T. Luu, F. Maldonado-Hodar, J. Rivera-Utrilla, and C. Moreno-Castilla, "Optimization of conditions for the preparation of activated carbons from olive-waste cakes," *Carbon*, vol. 39, pp. 425–432, 2001.
- [12] D. Mohan and K. P. Singh, "Single- and multi-component adsorption of cadmium and zinc using activated carbon derived from bagasse—an agricultural waste," *Water Research*, vol. 36, pp. 2304–2318, 2002.
- [13] H. S. Lee, J. H. Suh, I. B. Kim, and T. Yoon, "Effect of aluminum in two-metal biosorption by an algal biosorbent," *Minerals Engineering*, vol. 17, pp. 487–493, 2004.
- [14] C. V. Ortinero, A. P. B. Mariano, S. P. Kalaw, and R. R. Rafael, "Bioconversion of *Citrofortunella microcarpa* fruit waste into lactic acid by *Lactobacillus plantarum*," *Journal of Ecological Engineering*, vol. 18, pp. 35–41, 2017.
- [15] M. Y. T. Morte and L. H. Acero, "Potential of calamansi (*Citrofortunella microcarpa*) fruit peels extract in lowering the blood glucose level of *Streptozotocin* induced albino rats (*Rattus albus*)," *ETP International Journal of Food Engineering*, vol. 3, pp. 29–34, 2017.

- [16] P. E. Dim and M. Termtanun, "Treated clay mineral as adsorbent for the removal of heavy metals from aqueous solution," *Applied Science and Engineering Progress*, vol. 3, no. 3, pp. 511–524, 2021, doi: 10.14416/j.asep.2021.04.002.
- [17] Y. W. A. M. Akter and M. Z. Abedin, "Dyes removal from textile wastewater using orange peels," *International Journal of Science and Technology Research*, vol. 2, pp. 47–50, 2013.
- [18] D. E. P. Sumalapao, J. R. Distor, I. D. Ditan, N. T. S. Domingo, L. F. Dy, and N. R. Villarante, "Biosorption kinetic models on the removal of congo red onto unripe calamansi (*Citrus microcarpa*) peels," *Oriental Journal of Chemistry*, vol. 32, pp. 2889–2900, 2016.
- [19] F. Agboinghale, "Studies on the use of orange peel for adsorption of congo red dye from aqueous solution," *Computing, Information System, Development Informatics Allied Research Journal*, vol. 5, pp. 37–44, 2014.
- [20] Y. Wong, V. Moganaragi, and N. Atiqah, "Physico-chemical investigation of semiconductor industrial wastewater," *Oriental Journal of Chemistry*, vol. 29, no. 4, pp. 1421–1428, 2013.
- [21] U. Farooq, M. A. Khan, M. Athar, and J. A. Kozinski, "Effect of modification of environmentally friendly biosorbent wheat (*Triticum aestivum*) on the biosorptive removal of cadmium(II) ions from aqueous solution," *Chemical Engineering Journal*, vol. 171, pp. 400–410, 2011.
- [22] S. Kaur, S. Rani, and R. K. Mahajan, "Adsorption kinetics for the removal of hazardous dye congo red by biowaste materials as adsorbents," *Journal of Chemistry*, vol. 2013, 2013, doi: 10.1155/2013/628582.
- [23] C. X. Huang, M. J. Canny, K. Oates, and M. E. McCully, "Planning frozen hydrated plant specimens for SEM observation and EDX microanalysis," *Microscopy Research and Technique*, vol. 28, pp. 67–74, 1994.
- [24] G. S. Agarwal, H. K. Bhuptawat, and S. Chaudhari, "Biosorption of aqueous chromium(VI) by *Tamarindus indica* seeds," *Bioresource Technology*, vol. 97, pp. 949–956, 2006.
- [25] A. G. Prasad and M. A. Abdullah, "Biosorption of Fe (II) from aqueous solution using tamarind bark and potato peel waste: Equilibrium and kinetic studies," *Journal of Applied Science and Environmental Sanitation*, vol. 4, pp. 273–282, 2009.
- [26] B. S. Girgis, L. B. Khalil, and T. A. M. Tawfik, "Activated carbon from sugar cane bagasse by carbonization in the presence of inorganic acids," *Journal of Chemical Technology and Biotechnology*, vol. 61, pp. 87–92, 1994.
- [27] K. Banerjee, S. T. Ramesh, R. Gandhimathi, P. V. Nidheesh, and K. S. Bharathi, "A novel agricultural waste adsorbent, watermelon shell for the removal of copper from aqueous solutions," *Iranian Journal in Energy and Environment*, vol. 3, pp. 143–156, 2012.
- [28] Y. S. Ho and G. McKay, "A comparison of chemisorption kinetic models applied to pollutant removal on various sorbents," *Process Safety Environmental Protection*, vol. 76, pp. 332–340, 1998.
- [29] F. C. Wu, R. L. Tseng, and R. S. Juang, "Kinetic modeling of liquid-phase adsorption of reactive dyes and metal ions on chitosan," *Water Research*, vol. 35, pp. 613–618, 2001.
- [30] Y. S. Ho and G. McKay, "The kinetics of sorption of divalent metal ions onto sphagnum moss peat," *Water Research*, vol. 34, pp. 735–742, 2000.
- [31] P. Venkateswarlu, V. M. Ratnam, S. D. Rao, and V. M. Rao, "Removal of chromium from an aqueous solution using *Azadirachta indica* (neem) leaf powder as an adsorbent," *International Journal of Physical Sciences*, vol. 2, pp. 188–195, 2007.
- [32] K. A. Shroff and V. K. Vaidya, "Kinetics and equilibrium studies on biosorption of nickel from aqueous solution by dead fungal biomass of *Mucor hiemalis*," *Chemical Engineering Journal*, vol. 171, pp. 1234–1245, 2011.
- [33] I. Ullah, R. Nadeem, M. Iqbal, and Q. Manzoor, "Biosorption of chromium onto native and immobilized sugarcane bagasse waste biomass," *Ecological Engineering*, vol. 60, pp. 99–107, 2013.
- [34] R. Negi, G. Satpathy, Y. K. Tyagi, and R. K. Gupta, "Biosorption of heavy metals by utilizing onion and garlic wastes," *International Journal Environmental and Pollution*, vol. 49, p. 179, 2012.
- [35] K. Srividya and K. Mohanty, "Biosorption of hexavalent chromium from aqueous solutions by catla scales: Equilibrium and kinetics studies,"



- Chemical Engineering Journal*, vol. 155, pp. 666–673, 2009.
- [36] S. Çay, A. Uyanık, and A. Özaşık, “Single and binary component adsorption of copper(II) and cadmium(II) from aqueous solutions using tea-industry waste,” *Separation and Purification Technology*, vol. 38, pp. 273–280, 2004.
- [37] V. S. Mane, I. D. Mall, and V. C. Srivastava, “Use of bagasse fly ash as an adsorbent for the removal of brilliant green dye from aqueous solution,” *Dye and Pigments*, vol. 73, pp. 269–278, 2007.
- [38] N. Ayawei, A. T. Ekubo, D. Wankasi, and E. D. Dikio, “Adsorption of congo red by Ni/Al-CO₃: Equilibrium, thermodynamic and kinetic studies,” *Oriental Journal of Chemistry*, vol. 31, pp. 1307–1318, 2015.
- [39] S. Veli and B. Alyüz, “Adsorption of copper and zinc from aqueous solutions by using natural clay,” *Journal of Hazardous Materials*, vol. 149, pp. 226–233, 2007.
- [40] Z. Jabbar, A. Angham, and G. H. F. Sami, “Removal of azo dye from aqueous solutions using chitosan,” *Oriental Journal of Chemistry*, vol. 30, pp. 571–575, 2014.
- [41] Y. C. Wong, K. N. Ranjini, and W. A. W. Nurdiana, “Removal of congo red and acid yellow 36 dye using orange peel and rice husk as absorbents,” *Oriental Journal of Chemistry*, vol. 30 pp. 529–539, 2014.
- [42] M. R. Haris and K. Sathasivam, “The removal of methyl red from aqueous solutions using banana pseudostem fibers,” *American Journal of Applied Sciences*, vol. 6, p. 1690, 2009.
- [43] R. Mallampati and S. Valiyaveetil, “Application of tomato peel as an efficient adsorbent for water purification—alternative biotechnology?,” *RSC Advances*, vol. 2, 2012, Art. no. 9914.
- [44] A. S. K. Kumar, R. Ramachandran, S. Kalidhasan, V. Rajesh, and N. Rajesh, “Potential application of dodecylamine modified sodium montmorillonite as an effective adsorbent for hexavalent chromium,” *Chemical Engineering Journal*, vol. 1211–1212, pp. 396–405, 2012.
- [45] S. Pandey and S. B. Mishra, “Organic–inorganic hybrid of chitosan/organoclay bionanocomposites for hexavalent chromium uptake,” *Journal of Colloid and Interface Science*, vol. 361, pp. 509–520, 2011.